University of Groningen

Collective Optical Response of Molecular Aggregates

Fidder, H.

Published in:
Physica Status Solidi B

DOI:
10.1002/pssb.2221880126

IMPORTANT NOTE: You are advised to consult the publisher's version (publisher's PDF) if you wish to cite from it. Please check the document version below.

Document Version
Publisher's PDF, also known as Version of record

Publication date:
1995

Link to publication in University of Groningen/UMCG research database

Citation for published version (APA):
Fidder, H. (1995). Collective Optical Response of Molecular Aggregates. Physica Status Solidi B, 188(1).
DOI: 10.1002/pssb.2221880126

Copyright
Other than for strictly personal use, it is not permitted to download or to forward/distribute the text or part of it without the consent of the author(s) and/or copyright holder(s), unless the work is under an open content license (like Creative Commons).

Take-down policy
If you believe that this document breaches copyright please contact us providing details, and we will remove access to the work immediately and investigate your claim.

Downloaded from the University of Groningen/UMCG research database (Pure): http://www.rug.nl/research/portal. For technical reasons the number of authors shown on this cover page is limited to 10 maximum.

Download date: 10-02-2018

phys. stat. sol. (b) **188**, 285 (1995)

Subject classification: 63.50 and 78.30; 71.45; 78.55; S12

Ultrafast Laser and Spectroscopy Laboratory, Department of Chemical Physics, Materials Science Centre, University of Groningen [1])

Collective Optical Response of Molecular Aggregates

By

H. FIDDER [2]) and D. A. WIERSMA

Relative fluorescence quantum yield, fluorescence lifetime, optical dephasing, and absorption line shift data are presented for both excitonic transitions of the pseudoisocyanine (PIC) J-aggregate. The data indicate activation of the optical dephasing by exciton–acoustic phonon scattering at low temperatures. Above approximately 80 K the optical dephasing, line shift as well as the fluorescence lifetime lengthening call for activation by high frequency phonons. Moreover, resonance Raman data indicate the delocalization of low frequency vibrational modes in the aggregate.

1. Introduction

Molecular aggregates are mesoscopic clusters of molecules, with sizes intermediate between crystals and isolated molecules. Molecular aggregates belong to the group of nanostructure materials [1], which currently create much interest. In particular the unique optical properties of these materials receive special attention. Examples of nanostructures other than aggregates are quantum-wells and -dots [1], Langmuir-Blodgett films, and polymers [2]. An important difference between molecular aggregates and most other nanostructures is the absence of electron delocalization, which makes their optical response easier to model. On the other hand, a complicating factor in the study of aggregates is that there is virtually no control on their structure and composition, whereas quantum-wells and -dots can be built to fit nearly any physical specification.

The first observation of aggregate formation was made in 1936 independently by both Jelley [3] and Scheibe [4], on the dye molecule pseudoisocyanine (PIC), dissolved in water at high concentrations. A characteristic signature of aggregation is the rise of a narrow absorption band, the so-called J-band, which is considerably red-shifted relative to the molecular optical transition. It was later discovered by Cooper [5] that in a glass of water/ethylene glycol, at low temperatures, PIC-Br yields even six to seven times narrower bands than at room temperature. However, in this case two J-bands are observed, which have been assigned to two different aggregate structures [6].

A strong stimulus to the field of aggregate research was provided by the discovery that coherently coupled molecules show collective radiative dynamics [7 to 17]. This property has been referred to as exciton superradiance. A study of the fluorescence lifetime in PIC J-aggregates has been undertaken in the past by numerous authors [8 to 12]. In most experiments, however, too high light intensities were used, leading to a drastic shortening

[1]) Nijenborgh 4, NL-9747 AG Groningen, The Netherlands.

[2]) Present address: Department of Chemical Physics, University of Lund, P.O. Box 124, S-22100 Lund, Sweden.

of the fluorescence decay as a result of exciton–exciton annihilation [10, 11]. A temperature dependent fluorescence lifetime study of the PIC-Br aggregates in a water/ethylene glycol glass, under low excitation density conditions, was first performed by de Boer and Wiersma [12]. They found that at 1.5 K the fluorescence lifetime of the PIC aggregates was 50 times shorter than the radiative lifetime of the monomer. At higher temperatures the fluorescence lifetime lengthened, similar to what had been observed by Feldmann et al. [13] in GaAs/AlGaAs multiple quantum-wells (MQWs), which could be explained by thermalization of the excitonic population over the exciton band. The connection between exciton dephasing and fluorescence lifetime made by Feldmann et al. [13], and the photon echo study on PIC aggregates by de Boer et al. [6], motivated Mukamel and coworkers [14 to 17] to a theoretical investigation of the connection between superradiance and exciton dephasing in molecular aggregates. Using a microcopic description which included exciton–phonon coupling (for acoustic or optical phonons) they managed to give a description [16] of the temperature dependence of the fluorescence lifetime in fair agreement with the measurements of de Boer and Wiersma [12]. A key aspect of this description is that the exciton population should become non-Boltzmann at elevated temperatures.

In this paper the temperature dependencies of the fluorescence lifetime, the relative fluorescence quantum yield, the optical dephasing, and the J-band line shift are discussed for both J-bands (sites) of the PIC-Br J-aggregate. Fluorescence quantum yield measurements on the PIC J-aggregate have not been presented before, and are essential for interpreting the radiative dynamics. Furthermore, few data have been presented on the "blue site" so far. Moreover, we present and discuss resonance Raman results on both PIC aggregates and monomers that indicate that a number of vibrational modes are delocalized in the aggregate.

2. Experimental

Relative fluorescence quantum yield experiments were performed by excitation around 495 nm, with light from a halogen lamp that was passed through a 495 nm interference filter. The fluorescence was detected by an intensified optical multichannel analyzer diode array, mounted on Spex 1877 triplemate monochromator. During the experiments no elements of the set-up were adjusted or realigned. The fluorescence of both sites was detected simultaneously. This experimental approach was chosen, because a) direct excitation of the J-band causes hole-burning [6, 18], b) direct excitation of the J-band requires scanning, to get rid of laser straylight and Rayleigh scattering, making it harder to maintain the alignment stability, c) the J-band shifts and broadens with increasing temperature, so the absorption at a fixed wavelength changes with temperature [19]. Problems a) and c) are circumvented by the broad excitation bandwidth of ≈ 10 nm.

The time-correlated single photon counting (TCSPC) and accumulated photon echo (APE) set-ups and experiments have been described elsewhere [6, 12].

Resonance Raman measurements on the 576.1 nm (red site) excitonic transition of the PIC-Br aggregates were performed using a R6G dye laser, pumped by a cw argon ion laser operating on all lines. For the experiments on the monomer the 514.5 nm line of the cw argon ion laser was used. In both cases a Spex 1402 double monochromator equipped with a RCA C31034A-02 single photon counting tube was used for detection. Typical resolution was on the order of 0.5 cm^{-1}.

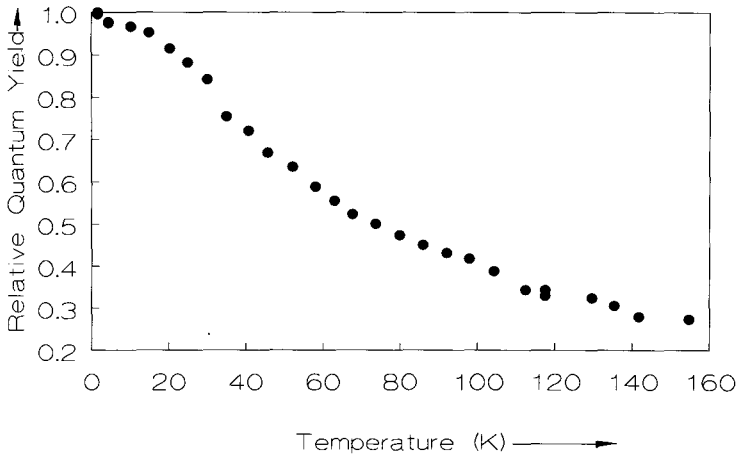

Fig. 1. Relative fluorescence quantum yield of PIC-Br J-aggregates vs. temperature (both sites show the same behaviour)

3. Radiative Decay and Optical Dephasing

The parameter that gives a good indication of the feasible enhancement of optical nonlinearities due to aggregation, is the increase of the radiative decay rate. The fluorescence lifetime of the red site of the PIC aggregate has been found to be 50 times shorter than the radiative lifetime of the monomers, and to lengthen significantly with rising temperatures [12]. Knowledge of the fluorescence quantum yield is essential to the determination of the radiative decay rate, and for a full understanding of its temperature dependence. We therefore have measured the relative fluorescence quantum yield of the PIC aggregates from 1.5 to 190 K. Fig. 1 shows the relative fluorescence quantum yields, of both sites together, as a function of temperature. An analysis of the data showed that the decrease of the fluorescence quantum yield, as a function of temperature, is the same for both sites. Fig. 1 shows that the quantum yield decreases more or less linear with temperature between 1.5 and 160 K, by a factor ≈ 3.6. Between 180 and 190 K an increase in fluorescence yield by a factor of three was observed, which we ascribe to a continuation of aggregation upon melting of the glass. Therefore data above 160 K are not included in Fig. 1.

The temperature dependence of the fluorescence lifetime of PIC-Br aggregates, between 1.5 and 160 K, corrected for the drop in relative fluorescence quantum yield, is depicted in Fig. 2. The quantum yield correction reduces the temperature up to which the fluorescence lifetime remains constant from 50 K [12, 19] to less than 30 K. In the description of the uncorrected data by Spano et al. [16], where dephasing was activated by a 240 nm^{-1} optical phonon, the constant regime up to 50 K was matched well due to negligible activation of the optical phonon up to this temperature. The lower on-set temperature of the radiative lifetime lengthening, due to the quantum yield correction, could be obtained by using a lower freqency optical phonon. The stronger increase of the relative radiative lifetime compared to the fluorescence lifetime could either indicate a stronger exciton–phonon coupling constant, or activation by an optical phonon of lower energy. Previously, we have concluded from resonance light scattering experiments that up to 77 K a thermalized excitonic population is maintained over the exciton band [20]. Since the oscillator strength

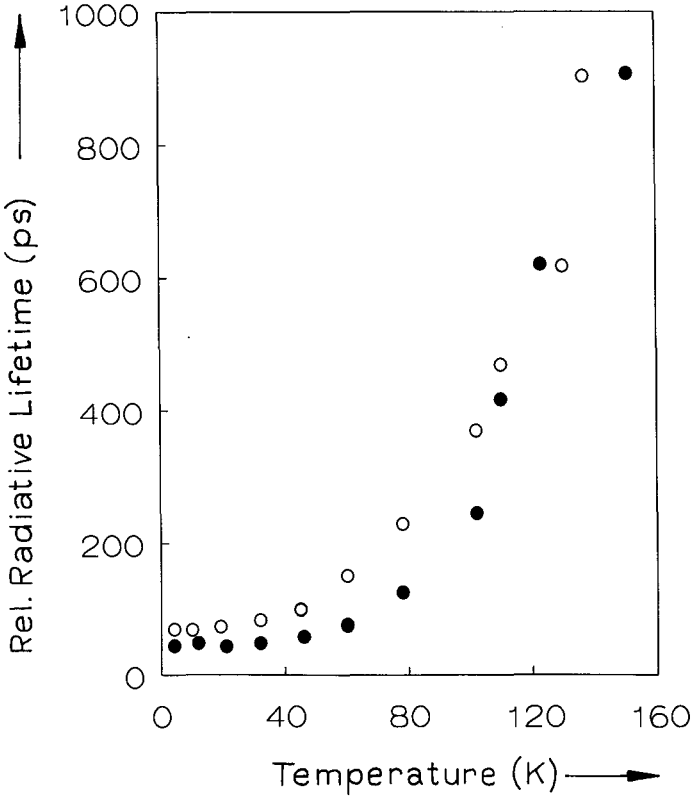

Fig. 2. Relative radiative decay time as a function of temperature for the blue (●, λ_{max} = 570.2 nm at 1.5 K) and red (○, λ_{max} = 576.1 nm at 1.5 K) excitonic J-bands of PIC-Br aggregates. Excitation was performed at 545 nm

is distributed over an energy width of only about 30 cm^{-1}, and since across this range the average oscillator strength per aggregate eigenstate decreases significantly [21], the radiative lifetime is expected to lengthen already somewhat even between 1.5 and 50 K. A full description of the fluorescence lifetime should thus include exciton-acoustic phonon scattering next to exciton–optical phonon scattering. However, the lengthening of the fluorescence lifetime, both before and after the relative quantum yield correction, remains far too strong above 70 K in order to be understood on the basis of a thermalized exciton population. Recently, we have found experimental evidence that suggests that indeed at higher temperatures the exciton population becomes non-thermal [22], as was invoked in the theoretical description by Spano et al. [16].

In Fig. 3 we show the temperature dependence of the total dephasing time T_2 for both sites. The low temperature accumulated photon echo decay is non-exponential [6]. At these temperatures we have taken the full width at half maximum (FWHM) of the Fourier transform of the coherence decay as a measure for the (effective) total dephasing time T_2. Above $\approx$100 K the dephasing times were extracted from the analysis of the absorption line shape [19]. For excitons on homogeneous linear chains and linear exciton–phonon coupling, the dephasing can be caused by phonon-induced modulation of the intermolecular resonance interaction. Davydov [23] argued that, if this coupling is small, its effect on the exciton

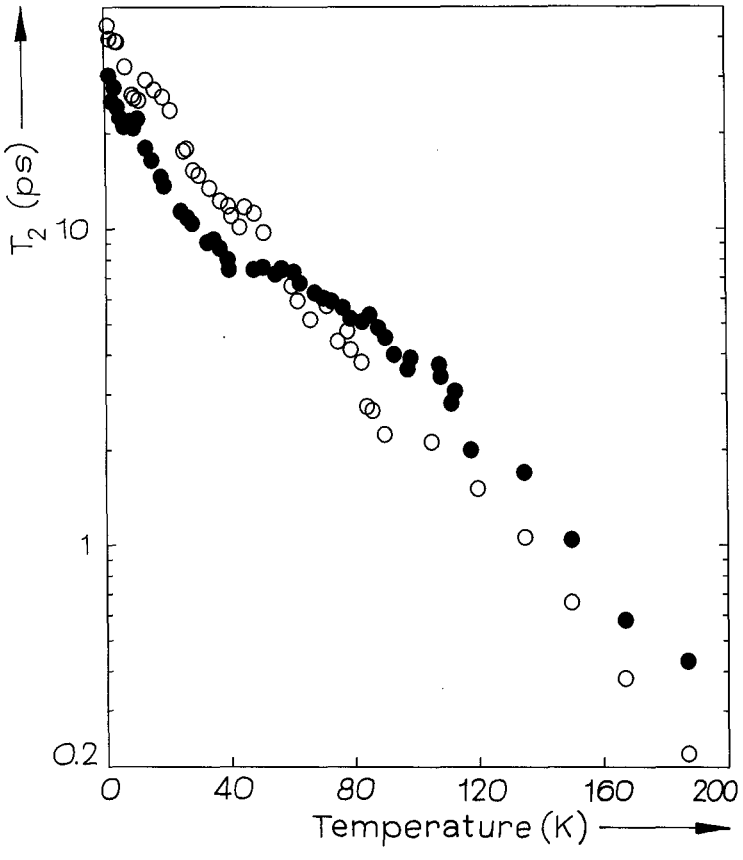

Fig. 3. The dephasing time T_2 as a function of temperature for both the blue (●) and red (○) excitonic origins of the PIC-Br aggregate. In the low temperature region an effective T_2 is derived from the echo decay

dynamics can be described in terms of elastic and inelastic scattering of excitons through the band. This phonon-induced exciton scattering process leads to both a temperature dependent line width and shift of the excitonic transition. Several authors [23 to 25] have shown that the frequency dependent homogeneous width $\Gamma(\boldsymbol{k}, \omega)$ and shift $\Delta(\boldsymbol{k}, \omega)$ take the following form for the case of linear exciton–phonon coupling and second-order perturbation theory in the exciton–phonon coupling:

$$\Gamma(\boldsymbol{k}, \omega) = \frac{2\pi}{N} \sum_{qs} |F_s(\boldsymbol{k}, \boldsymbol{q})|^2 \times \{n_{qs}\delta[\omega - E(\boldsymbol{k} + \boldsymbol{q}) + \Omega_s(\boldsymbol{q})] + (n_{qs} + 1)\,\delta[\omega - E(\boldsymbol{k} + \boldsymbol{q}) - \Omega_s(\boldsymbol{q})]\}\,, \tag{1a}$$

$$\Delta(\boldsymbol{k}, \omega) = \frac{P}{N} \sum_{qs} |F_s(\boldsymbol{k}, \boldsymbol{q})|^2 \times \left\{\frac{n_{qs}}{[\omega - E(\boldsymbol{k} + \boldsymbol{q}) + \Omega_s(\boldsymbol{q})]} + \frac{(n_{qs} + 1)}{[\omega - E(\boldsymbol{k} + \boldsymbol{q}) - \Omega_s(\boldsymbol{q})]}\right\}. \tag{1b}$$

Here $F_s(\boldsymbol{k}, \boldsymbol{q})$ is the exciton–phonon interaction matrix element for an exciton with wave vector $\boldsymbol{k}$ and a phonon of branch s with wave vector $\boldsymbol{q}$. n_{qs} is the thermal (Bose-Einstein) occupation number for phonons, $E(\boldsymbol{k} + \boldsymbol{q})$ is the energy of the exciton after scattering, and $\Omega_s(\boldsymbol{q})$ is the phonon energy. N is the number of molecules that are coherently coupled and P in (1b) denotes the principal value. The terms in (1) containing the factor n_{qs} $(n_{qs} + 1)$ describe absorption (emission) of a phonon with wave vector $\boldsymbol{q}$ by the exciton. When higher-order perturbation theory is used, or higher-order exciton–phonon processes are taken into account the expressions for $\Gamma(\boldsymbol{k}, \omega)$ and $\Delta(\boldsymbol{k}, \omega)$ become more complex, but again homogeneous width and shift of the excitons are related to exciton–phonon scattering processes.

The temperature dependence of the homogeneous line width of the red site can be described by thermal (Bose-Einstein) activation of exciton–phonon scattering based on (1a), using three phonons of $9\,\mathrm{cm}^{-1}$ $(0.3\,\mathrm{cm}^{-1})$, $305\,\mathrm{cm}^{-1}$ $(153\,\mathrm{cm}^{-1})$ and $973\,\mathrm{cm}^{-1}$ $(49\,500\,\mathrm{cm}^{-1})$, respectively. The numbers between parentheses are the prefactors, associated with the exciton–phonon coupling parameter $|F(\boldsymbol{k}, \boldsymbol{q})|^2$ for these modes. As the fit is merely an effective description of the data, not too much physical significance should be attached to the actual frequencies. The onset of a strong high-frequency dephasing channel was also observed by Hirschmann and Friedrich [26] in hole-burning experiments on PIC-I aggregates. Previously, the low frequency $(9\,\mathrm{cm}^{-1})$ value was assigned to a specific mode [6, 26] (phonon or libration). This interpretation was shown to be erroneous by resonance light scattering experiments [19, 20], which showed that *all* thermally populated phonons contribute to the dephasing. Apparently, in disordered systems the condition of conservation of momentum does not impose a strong limitation to the energy of the phonons that are active in the exciton–phonon scattering process. Recently, we demonstrated that both the wavelength and temperature dependent dephasing data of a different type of aggregate can be described in terms of exciton–phonon scattering, using phonons of all frequencies [27]. There is a strong correlation between the exciton dephasing and fluorescence lifetime (verify [19]). Noteworthy is also the fact that the value of the second phonon in the "dephasing fit" of $305\,\mathrm{cm}^{-1}$, is close to the optical phonon (vibration) of $240\,\mathrm{cm}^{-1}$ used by Spano et al. [16] to fit the temperature dependence of the fluorescence lifetime. The coupling constant of this phonon, on the other hand, is off by nearly a factor three $(153/2 = 76.5\,\mathrm{cm}^{-1}$, compared to $210\,\mathrm{cm}^{-1}$ [16]).

It is interesting to observe that, whereas the low temperature echo decay of the blue site is nearly two times faster than for the red site, at high temperatures the red site dephases twice as fast. The low temperature difference is not caused by the transfer of population from the blue to the red site. We have estimated this to be approximately 10% [22], which is too little to explain the difference in low temperature dephasing. A rather qualitative conclusion from the data in Fig. 3 is that the coupling to (low frequency) phonons is stronger for the blue site, whereas the coupling to optical phonons (presumably vibrations) is strongest for the red site. It has been concluded that the blue site aggregate structure is thermodynamically preferred [6]. The difference in exciton–phonon coupling strengths for both low and high temperature regimes might therefore be caused by differences in the aggregate structure or by different micro-environments of the two structures.

Aside from a broadening, (1) also predicts a shift of the absorption band. Contrary to the line broadening, the shift contains contributions from non-resonant terms too, and it is therefore hard to predict its temperature dependence. For both sites of the PIC-Br aggregate, we have observed a band shift with rising temperature. These results are depicted

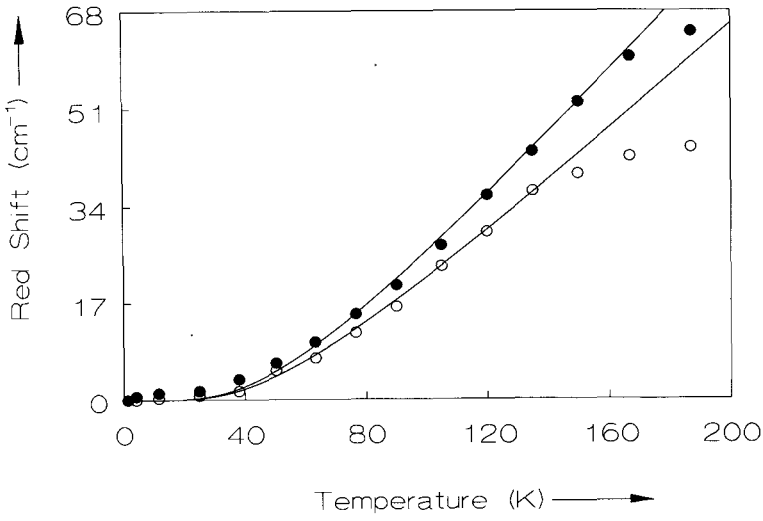

Fig. 4. Temperature dependence of the line shift of the blue (●) and red (○) site J-bands of the PIC-Br aggregate together with fits based on Bose-Einstein activation of the shift by a single phonon. In both cases the phonon energy is 100 cm^{-1}, the coupling (pre-)factor is 83 cm^{-1} for the blue and 71 cm^{-1} for the red site

in Fig. 4. Both sites show a red shift, which levels off at ≈ 135 K for the red site and ≈ 170 K for the blue site. The shift of the two J-bands can be described by a Bose-Einstein activation process involving a 100 cm^{-1} phonon. The prefactor is somewhat larger for the blue site, i.e., 83 cm^{-1} compared to 71 cm^{-1} for the red site. Note that a coupling strength of 71 cm^{-1} agrees well with the coupling value of 76.5 cm^{-1} for the second phonon in the fit to the dephasing data. Note furthermore that the band shift suggests that the blue site couples stronger to vibrations, contrary to what the dephasing data show at higher temperatures. This should be taken as an illustration of the uncertainty in the analysis of the band shifts. The levelling off of the shift is not understood. Equation (1b), however, does not exclude the possibility of contributions that could cause a blue-shift. An intriguing possibility is that, at this temperature, dephasing starts to affect the delocalization length. This is to be expected if dephasing prevents a coherent coupling over the delocalization length, as determined by the ratio of the disorder over the interaction D/J [21]. In absorption measurements on mixed aggregates we have observed that a decrease in the delocalization length, while maintaining the same disorder/interaction energy ratio (D/J), results in a blue-shift of the J-band [22]. For the red site in the aggregate of PIC-Br the 1.5 K coherence (delocalization) length is on the order of 50 molecules and the dipolar nearest-neighbour coupling energy is about -600 cm^{-1} [21, 28]. The transfer frequency between neighbouring molecules in the aggregate, associated with this coupling of -600 cm^{-1} is 72 THz. So it will take about 1.3 ps for the exciton to move once coherently back and forth on the chain. The dephasing time at 135 K is 1.1 ps. These numbers suggest that a reduction of the size of the coherence domain by dephasing is possible at high temperatures. The argumentation used is, however, very simplistic and does not explain quantitatively the difference in the onset temperature for the levelling off of the two sites. Although the fact that the levelling off occurs at a lower temperature for the red site than for the blue site is predicted by the above argument.

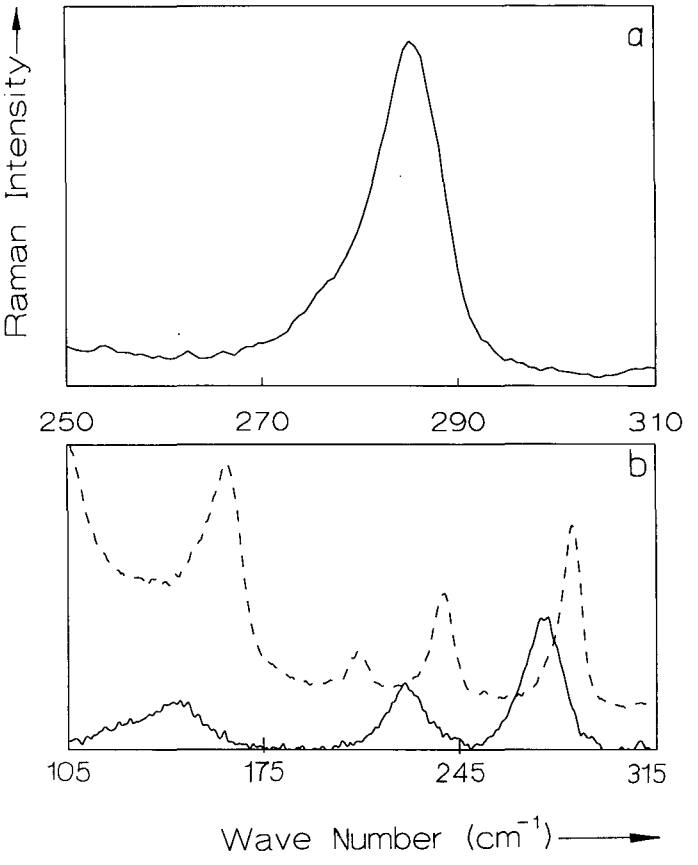

Fig. 5. a) The 285 cm^{-1} mode in the 1.5 K J-aggregate Raman spectrum. b) The low frequency part of the PIC-Br aggregate (-----, measured at 1.5 K) and monomer (———, measured at room temperature) Raman spectrum. The large fluorescence background in the monomer spectrum has been substracted. For details pertaining to the analysis of the spectra see the text and Table 1

4. Observation of Vibron Bands

When we measured the Raman spectrum of the PIC aggregate at 1.5 K (for instance, see [19]), the low frequency modes were found to have asymmetric line shapes, similar to the J-band (verify, e.g. [20], Fig. 1). This is shown for the 285 cm^{-1} Raman band in Fig. 5a. Note that the Lorentzian tail is towards *lower* (vibrational) energy. Because of the similarity with the line shape of the J-band, the question arises if this means that also the ground state vibrations, which are mapped by the Raman technique, are delocalized. If this is the case, then the Raman lines of the aggregate should be shifted relative to the PIC monomer Raman spectrum, due to interactions. In Fig. 5b the low frequency part of the Raman spectra of the aggregate (at 1.5 K, excited at 577.1 nm) and monomer (at room temperature in 1 : 1 water/ethylene glycol, excited at 514.5 nm) are shown. The fluorescence background in the monomer spectrum has been substracted. Because the monomer signals are broad and the fluorescence background rises steeply, the line shapes of the monomer spectrum are not very accurately determined. The weak 208 cm^{-1} mode could not be discovered in

Table 1
Characteristics of PIC monomer and aggregate low frequency vibrational modes

ν_{mon} (cm^{-1})	$FWHM_{mon}$ (exp.) (cm^{-1})	ν_{agg} (cm^{-1})	$FWHM_{agg}$ (cm^{-1})	f (cm^{-1})	d/f	$FWHM_{mon}$ (calc.) (cm^{-1})
142 ± 5	34 ± 5	162 ± 2	13 ± 2	+8.1	1.3	26
		208 ± 2	8 ± 1			
226 ± 2	17 ± 2	239 ± 2	7 ± 1	+5.5	1.1	15
276 ± 2	18 ± 2	285 ± 1	7 ± 1	+3.5	1.6	13
422 ± 2	13 ± 2	424 ± 2	6 ± 1			

the monomer spectrum. It is, however, very clear from Fig. 5b that the aggregate vibrational frequencies are indeed shifted to higher frequencies. In Table 1 the frequencies and the full width at half maximum (FWHM) of the first five Raman lines are given. The positions of the Raman lines from 422 cm^{-1} up are equal in the monomer and aggregate spectra, within experimental accuracy.

The delocalization of the vibrations is caused by an exchange coupling f_{mn}. In analogy to the Frenkel exciton states of the electronic transition, we can describe the vibrations as delocalized states: vibrons. The framework of [21] for the description of exciton states can be applied to these vibron states as well with the replacement of D by d, the vibrational energetic disorder, and J by f, the nearest-neighbour interaction for the vibrational transition. Because the nature of the interaction is not known we will restrict ourselves to nearest-neighbour coupling only in the analysis. A full analysis with nearest-neighbour interactions has not been made by us, so we use the coherent potential approximation results of Boukahil and Huber [29] in our analysis of the monomer and aggregate Raman spectra. The dependencies Boukahil and Huber [29] found for the full width at half maximum and the shift of the band are $1.09f(d/f)^{4/3}$ and $0.315f(d/f)^{4/3}$, respectively. The homogeneous shift by the interactions is $2f$ when using only nearest-neighbour interactions. The values of f and d/f obtained from combining the energy shift and the FWHM of the aggregate Raman lines are given in Table 1 for the three modes for which such an analysis is possible. Also we give the width of the monomer band as predicted, *a posteriori*, from the values of d and f. The agreement of these widths with experiment is fairly good. Note that disorder on electronic (D) and vibrational (d) transitions are not expected to be mutually correlated.

From Table 1 we find that, contrary to the electronic transition, the vibrational transitions have a positively valued interaction. At this point it is important to note that the resonance enhancement by the $k = 0$ (J-band) exciton state results in the observation of the $q = 0$ vibron (delocalized vibration) state in the Raman spectrum [22]. The blue-shift of the aggregate Raman lines therefore implies that the vibrational interactions have a sign opposite from the electronic interactions. One-dimensional vibron bands have previously been observed in crystals of 1,2,4,5-tetrachlorobenzene by Abramson et al. [30], by resolving the spectral structure of the phosphorescence emission from the triplet exciton band to the ground state vibron bands as a function of temperature. A theoretical analysis of the band structure in these crystals was performed by Jongenelis et al. [31] by means of lattice dynamics calculations, in which the intermolecular interactions are determined by analytical atom–atom potentials. The largest vibron band in this crystal corresponds to a coupling constant f of about 4 cm^{-1}, which is of comparable size as the couplings observed by us. Jongenelis et al. [31] conclude that inclusion of partial charges on atoms in the calculations is necessary for obtaining the correct vibron band widths, and also that the sign of the exchange

interaction is determined by the sign of the charges on the atoms active in the vibration of interest. Both these conclusions are, however, poorly substantiated by the experimental and calculated data: Of the only three vibron bands with experimental widths larger than the experimental resolution one cannot at all be described by the calculations and one has a band width nearly a factor two larger than given by the calculations. For two of these three bands no measurable splitting is calculated without the additional charges; for the third band the inclusion of charges increased the calculated band width but did not determine the sign of the interaction. Apparently these lattice dynamics calculations are not on a quantitative level of description yet. Based on the laws of electrostatics one would also not expect a difference in sign for interactions between two positive or negative charges. A better statement would have been that charges also influence the size of vibron band widths. For PIC this could imply that vibron bands are formed for vibrations which involve the positively charged nitrogen atoms. A noticeable result from the calculations by Jongenelis et al. [31] is that no significant vibron band formation ($f > 1\ \mathrm{cm}^{-1}$) is found above $\nu = 400\ \mathrm{cm}^{-1}$, which agrees with our observations.

The ratios of d/f in Table 1 are large compared to the ratios which describe the excitonic J-band ($D/J = 0.106$) [19]: Therefore the disorder contribution to the vibron band shift (a blue-shift because of the positive value of f) is considerable. Because the ratio d/f is an order of magnitude larger than the D/J ratio, the delocalization length of the vibrons is expected to be significantly less than the exciton delocalization.

5. Summary

We have observed a linear decrease with temperature of the fluorescence quantum yield of PIC aggregates, by a factor 3.6 between 1.5 and 160 K, for both sites. At the same time the fluorescence lifetime is found to lengthen significantly with rising temperature. Both fluorescence lifetime, optical dephasing, and absorption line shift are mainly activated by high frequency optical phonons (presumably vibrations) above approximately 80 K, presumably leading to a non-thermal exciton population. Line shift data suggest further that the exciton coherence length is affected by the ultrafast optical dephasing at high temperatures (>135 K for the red site, >170 K for the blue site). At low temperatures (<70 K) exciton dephasing is mainly governed by exciton–acoustic phonon scattering, and the exciton population is thermalized. Furthermore, we have found evidence for the existence of vibron (vibrational exciton) bands in the molecular aggregate of PIC.

Acknowledgements

We thank Jasper Knoester for many interesting discussions on molecular aggregates. We are grateful to Foppe de Haan for providing software for instrument control and data analysis. This research was supported by the Netherlands Foundation for Chemical Research (SON), with financial aid from the Netherlands Organization for the Advancement of Science (NWO).

References

[1] Physics Today **46**, No. 6 (1993).
[2] J. phys. Chem. **96**, No. 7 (1992).
H. KIESS (Ed.), Conjugated Conducting Polymers, Springer-Verlag, Berlin 1992.
[3] E. E. JELLEY, Nature (London) **138**, 1009 (1936); **139**, 631 (1937).
[4] G. SCHEIBE, Angew. Chem. **49**, 563 (1936); **50**, 212 (1937).

[5] W. Cooper, Chem. Phys. Letters **7**, 73 (1970).
[6] S. de Boer, K. J. Vink, and D. A. Wiersma, Chem. Phys. Letters **137**, 99 (1987).
[7] R. H. Lehmberg, Phys. Rev. A **2**, 883 (1970).
[8] S. K. Rentsch, R. V. Danielius, R. A. Gadonas, and A. Piskarskas, Chem. Phys. Letters **84**, 446 (1981).
[9] B. Kopainsky and W. Kaiser, Chem. Phys. Letters **88**, 357 (1982).
[10] V. Sundström, T. Gillbro, R. A. Gadonas, and A. Piskarskas, J. chem. Phys. **89**, 2754 (1988).
[11] D. V. Brumbaugh, A. A. Muenter, W. Knox, G. Mourou, and B. Wittnerhaus, J. Lum. **31**, 783 (1984).
[12] S. de Boer and D. A. Wiersma, Chem. Phys. Letters **165**, 45 (1990).
[13] J. Feldmann, G. Peter, E. O. Göbel, P. Dawson, K. Moore, C. Foxon, and R. J. Elliott, Phys. Rev. Letters **59**, 2337 (1987).
[14] F. C. Spano and S. Mukamel, Phys. Rev. **A 40**, 5783 (1989).
[15] F. C. Spano and S. Mukamel, J. chem. Phys. **91**, 683 (1989).
[16] F. C. Spano, J. R. Kuklinski, and S. Mukamel, Phys. Rev. Letters **65**, 211 (1990).
[17] F. C. Spano, J. R. Kuklinski, and S. Mukamel, J. chem. Phys. **94**, 7534 (1991).
[18] R. Hirschmann, J. Friedrich, and E. Daltrozzo, J. chem. Phys. **91**, 7296 (1989).
[19] H. Fidder, J. Terpstra, and D. A. Wiersma, J. chem. Phys. **94**, 6895 (1991).
[20] H. Fidder and D. A. Wiersma, Phys. Rev. Letters **66**, 1501 (1991).
[21] H. Fidder, J. Knoester, and D. A. Wiersma, J. chem. Phys. **95**, 7880 (1991).
[22] H. Fidder and D. A. Wiersma, in preparation.
[23] A. S. Davydov, Theory of Molecular Excitons, Plenum Press, New York 1971.
[24] Y. Toyozawa, Progr. theor. Phys. **20**, 53 (1958).
[25] D. P. Craig and L. A. Dissado, Chem. Phys. **14**, 89 (1976).
[26] R. Hirschmann and J. Friedrich, J. chem. Phys. **91**, 7988 (1989).
[27] H. Fidder and D. A. Wiersma, J. phys. Chem. **97**, 11603 (1993).
[28] B. Kopainsky, J. K. Hallermeier, and W. Kaiser, Chem. Phys. Letters **83**, 498 (1981).
[29] A. Boukahil and D. L. Huber, J. Lum. **45**, 13 (1990).
[30] E. H. Abramson, A. P. J. M. Jongenelis, and J. Schmidt, J. chem. Phys. **87**, 3719 (1987).
[31] A. P. J. M. Jongenelis, T. H. M. van den Berg, A. P. J. Jansen, J. Schmidt, and A. van der Avoird, J. chem. Phys. **89**, 4023 (1988).

(Received November 7, 1994)